

**Identifying sources of infiltration and inflow in sanitary sewers in a northern community
comparative assessment of selected methods**

Panasiuk, Oleksandr; Hedström, Annelie; Langeveld, Jeroen; Viklander, Maria

DOI

[10.2166/wst.2022.151](https://doi.org/10.2166/wst.2022.151)

Publication date

2022

Document Version

Final published version

Published in

Water science and technology : a journal of the International Association on Water Pollution Research

Citation (APA)

Panasiuk, O., Hedström, A., Langeveld, J., & Viklander, M. (2022). Identifying sources of infiltration and inflow in sanitary sewers in a northern community: comparative assessment of selected methods. *Water science and technology : a journal of the International Association on Water Pollution Research*, 86(1), 1-16. <https://doi.org/10.2166/wst.2022.151>

Important note

To cite this publication, please use the final published version (if applicable).
Please check the document version above.

Copyright

Other than for strictly personal use, it is not permitted to download, forward or distribute the text or part of it, without the consent of the author(s) and/or copyright holder(s), unless the work is under an open content license such as Creative Commons.

Takedown policy

Please contact us and provide details if you believe this document breaches copyrights.
We will remove access to the work immediately and investigate your claim.

Identifying sources of infiltration and inflow in sanitary sewers in a northern community: comparative assessment of selected methods

Oleksandr Panasiuk ^{a,*}, Annelie Hedström  ^a, Jeroen Langeveld  ^{b,c} and Maria Viklander  ^a

^a Department of Civil, Environmental and Natural Resources Engineering, Luleå University of Technology, Luleå 971 87, Sweden

^b Department of Water Management, TU Delft, AA Delft 2600, The Netherlands

^c Partners4UrbanWater, MJ Nijmegen 6524, The Netherlands

*Corresponding author. E-mail: oleksandr.panasiuk@ltu.se

 OP, 0000-0003-3591-3689; AH, 0000-0001-9541-3542; JL, 0000-0002-0170-6721; MV, 0000-0003-1725-6478

ABSTRACT

Infiltration and inflow (I/I) into sanitary sewers causes numerous negative effects on the whole wastewater management system and ultimately, on the receiving waters. Consequently, a number of methods have been developed to analyse the performance of sewer systems with respect to I/I, including: distributed temperature sensing (DTS), closed-circuit television (CCTV) inspections, flow and conductivity measurements, automatic or grab sampling of ammonium, smoke testing, and visual inspection of manholes. Such methods were compared in an application to sanitary sewers in a small community and assessed with respect to their accuracy and ability to identify locations of sources of I/I, as well as temporal and spatial resolutions of the obtained results. Furthermore, different approaches to ammonium sampling during I/I monitoring campaigns were discussed. It was concluded that among the methods tested in this study, DTS had the highest temporal and spatial resolution, while ammonium grab sampling showed promise for initial screening of large catchments.

Key words: ammonium, closed-circuit television inspection, conductivity, distributed temperature sensing, infiltration and inflow, wastewater

HIGHLIGHTS

- Number of methods to analyse I/I in sewer system were compared.
- CCTV and visual inspection provided many locations with a potential risk of I/I but were not confirmed by other methods.
- Advantages and practical limitations of different ammonium sampling strategies were discussed.
- Combination of two to three methods is recommended depending on the main focus of an I/I monitoring programme.

INTRODUCTION

Infiltration and inflow (I/I) into sanitary and combined sewers impair operation of sewer systems by reducing the effective capacity of sewers, increasing the risk of basement flooding and sanitary and combined sewer overflows (SSOs and CSOs). I/I impose additional non-sewage flows onto wastewater treatment plants (WWTPs) and thereby reduce their treatment efficiency. These factors increase operational costs of the whole sewer system (Karpf & Krebs 2011; Cahoon & Hanke 2017; Sola *et al.* 2020).

Causes of I/I entry into sewers are numerous and typically include misconnected roof or basement drains, broken pipes, leaking manholes, broken or missing manhole covers, submerged ventilation openings in manhole covers, and leaking pipe connections (Field & O'Connor 1997; Staufer *et al.* 2012; Sola *et al.* 2020). There are a number of pathways followed by I/I, depending on local conditions and climate: continuous infiltration of groundwater into sewers, inflow of rainfall or snowmelt runoff, and rainfall or snowmelt-induced infiltration due to temporally elevated groundwater tables following rain and snowmelt events. Ingress of extraneous water attributed to snowmelt is especially important in cold climate regions, such as Canada, northern USA and Scandinavia (Field & O'Connor 1997; Wright *et al.* 2006; Wittenberg & Aksoy 2010; Staufer *et al.* 2012).

This is an Open Access article distributed under the terms of the Creative Commons Attribution Licence (CC BY-NC-ND 4.0), which permits copying and redistribution for non-commercial purposes with no derivatives, provided the original work is properly cited (<http://creativecommons.org/licenses/by-nc-nd/4.0/>).

The planning of sewer rehabilitation to reduce I/I requires identification of I/I sources, with respect to locations or pathways, and measurement of I/I flow rates (Field & O'Connor 1997; Schilperoort *et al.* 2013). For estimating I/I volumes, the most suitable methods are those based on analysis of reference flows, or wastewater quality parameters, such as nutrients, electrical conductivity, etc. (De Bénédictis & Bertrand-Krajewski 2005; Mattsson *et al.* 2016; Cahoon & Hanke 2017; Zhang *et al.* 2018b). On the other hand, closed-circuit television (CCTV), visual and smoke inspections provide better information regarding the locations of I/I entry into sewers (Schweiger & Hassell 2004; Mattsson *et al.* 2016). Additionally, distributed temperature sensing (DTS) has the potential to both detect and locate I/I (Schilperoort *et al.* 2013; Panasiuk *et al.* 2015; Beheshti & Sægrov 2019).

The abovementioned methods for I/I monitoring can be applied at a range of scales, spanning from a catchment scale (e.g. reference flow methods) down to a detailed scale with a resolution in metres or decimetres (e.g., DTS or CCTV). Likewise, different methods provide results in different time scales, ranging from the timing of a single manual grab sample (e.g., ammonium concentration) to online readings (e.g., conductivity, DTS). A comparison of the available I/I methods should lead to a better understanding of their advantages and limitations, under specific conditions, and should facilitate the selection of a sequence of methods maximising the efficiency of an I/I monitoring strategy.

The aim of this paper is to evaluate and compare the selected methods (DTS, CCTV, flow rate measurements, manual grab sampling or automatic sampling of ammonium concentrations, on-line conductivity measurements, visual and smoke inspections). These methods are assessed with respect to their performance in identifying, locating and volumetrically quantifying I/I into sanitary sewers before, during and after the snowmelt period, under dry and wet weather conditions. Such comparative evaluations were done in the context of temporal and spatial resolutions of the selected methods.

MATERIALS AND METHODS

Study area

The study was conducted in a village of about 400 inhabitants, located near the town of Skellefteå with 35,000 inhabitants, in Northern Sweden, in 2015. Stormwater from the study area is drained mostly via open drainage swales. Wastewater is drained via a simple sewer system comprising an upstream pumping station (P8A), 2.3 km of the main sewer section (the thick line in Figure 1(a)), several short lateral sewers discharging to the main sewer section (thin lines in Figure 1(a)), and a downstream pumping station (P3A). The main sewer section comprised mostly concrete and PVC pipes 225–300 mm in diameter, and lateral sewers comprised concrete and PVC pipes 150–225 mm in diameter at the downstream end, where they drain into the main sewer. More information about the study area can be found in Panasiuk *et al.* (2019).

Experimental setup and instrumentation

The evaluation period was between 20 March, with the snow cover still present on the ground, and 3 June 2015. This period was chosen to evaluate methods under varying weather conditions before, during and after the snowmelt period.

DTS

The DTS measurements were performed using 3.2 km of fibre optic cable installed along the invert of the main sewer section ((A)-(E), Figure 1(a)) and in five lateral sewers, in the form of cable loops, marked L1–L5 in Figure 1(a). The temporal and spatial resolutions of the temperature measurements were 14 seconds and 0.25 m, respectively. For more details concerning the DTS installation setup see Panasiuk *et al.* (2019).

CCTV, smoke, dye and visual inspections

CCTV inspections were performed in August 2015 by an authorised CCTV inspector from the municipality, following the guidelines recommended by the Swedish Water & Wastewater Association (Svenskt Vatten 2006). The inspection covered the same sewers where the DTS was installed, as well as some additional tributary sewers. Protocols of the CCTV inspection were used as an input to this study. Locations classified in protocols as cracked pipes, root penetrations and visible inflows were double checked on the video.

Smoke, dye and visual inspections were performed by a certified third-party company in September 2016 and covered the whole wastewater sewer system, including manholes in the study area.

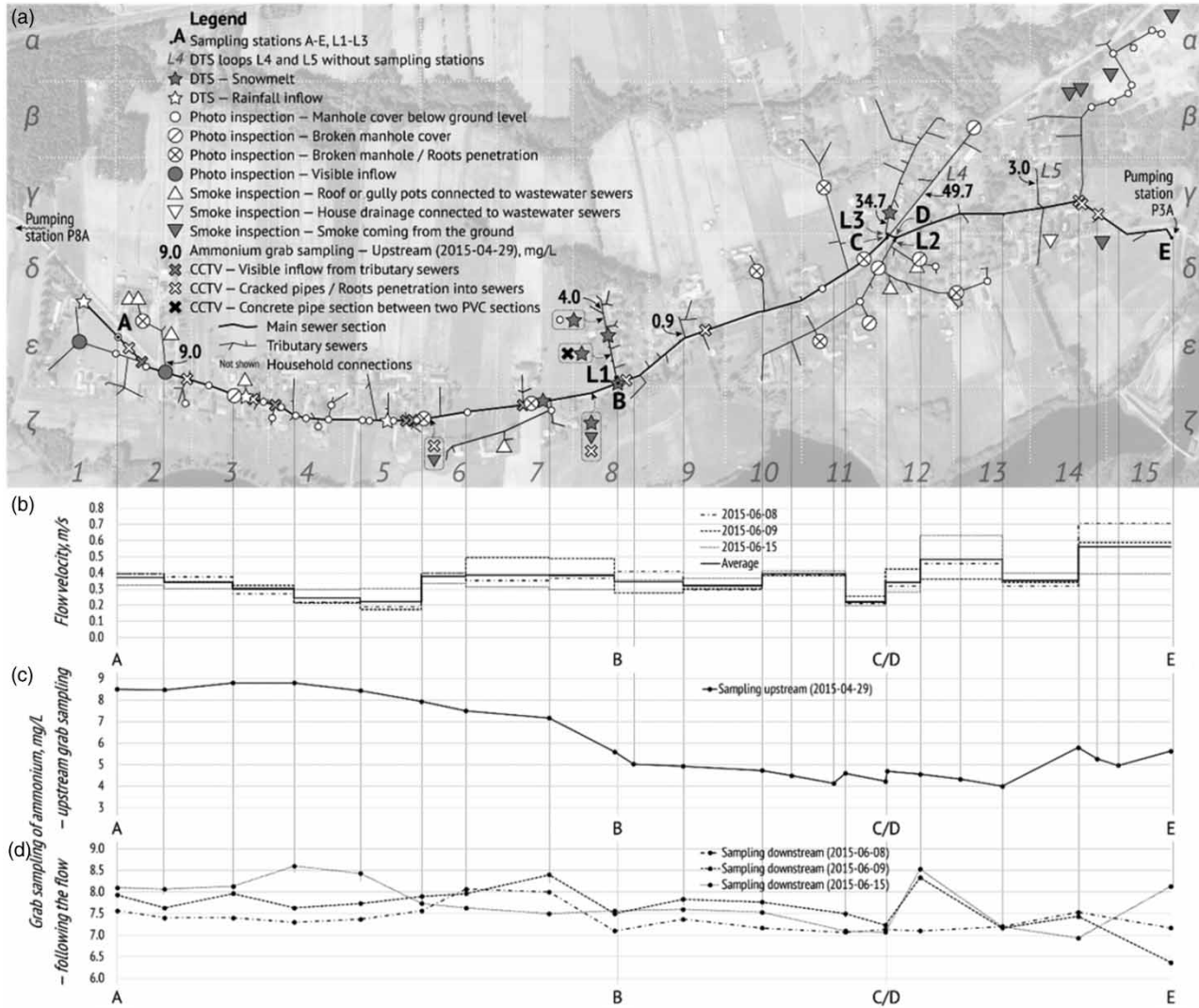


Figure 1 | (a) Results from DTS, CCTV, photo (visual) and smoke inspection, and ammonium grab sampling in tributary sewers plotted along the main sewer section (bold lines) and tributary sewers (thin lines) of the study section; (b) estimated flow velocities on 8, 9 and 15 June, and their averages (solid line); (c) analysed ammonium concentrations based on grab sampling on 29 April; (d) analysed ammonium concentrations based on Lagrangian sampling following the flow on 8, 9 and 15 June. Both (c) and (d) present average values for triplicate sampling and are plotted along the main sewer section with vertical lines connecting results with their corresponding locations. Note the difference in Y-scale between (c) and (d).

Ammonium sampling

Water samples to be analysed for ammonium were collected in three different ways: (a) by automatic samplers, (b) by manual sampling (called in this paper ‘upstream grab sampling’) and (c) by Lagrangian sampling, which followed the sewer flow (Barber *et al.* 2011), further explained below. All samples were analysed with respect to the ammonium concentrations, using QuAatro Applications Method No. Q-001-04 Rev. 0.

Ammonium sampling using automatic sampler. Automatic sampling for ammonium analyses was performed at eight sampling sites – five sites along the main sewer section (A, B, C, D and E) and three sites in the tributary sewers (L1, L2 and L3) (Figure 1(a)). Portable ISCO 6712 automatic samplers were used to collect four subsamples every 15 min into one bottle for obtaining a 1 h time-weighted sample. Seven sampling campaigns were performed (four of them lasted 24 hours and three lasted 48 hours), covering the snowmelt period, rain events and a dry weather period.

Ammonium grab sampling. In the upstream grab sampling, 87 samples were taken in triplicate from 29 manholes along the sewer section studied at the end of a dry weather period on 29 April, with 60 antecedent dry hours. The first sample was collected at the downstream station E and the remaining samples were collected while gradually moving upstream towards station A (Figure 1(a)). Samples were collected both from the main sewer section (Figure 1(c)) and from some tributary sewers (L1, L3, L4, L5 and two households' connection pipes) (Figure 1(a)).

Grab sampling was also performed by using Lagrangian sampling, in which the same 'parcel' of water is followed and sampled. Lagrangian sampling started at the upstream end of the main sewer section, releasing dye into the sewer at station A, and then collecting samples in triplicates at 17 downstream locations, as the peaks in dye colour arrived at, and were observed in, downstream manholes. The main advantages of Lagrangian sampling include minimisation of variability associated with daily cycles in sewage quality, and the possibility of quantitative mass-flow analysis in conjunction with flow rate measurements (Barber *et al.* 2011). This type of sampling of dry weather flows was conducted on three occasions on 8, 9 and 15 June (Figure 1(d)), with antecedent dry weather periods of 1, 2 and 8 antecedent days, respectively, starting at 14:00, with the last sample collected at 15:46 ± 1 min.

Electrical conductivity

Eight sampling stations, A–E and L1–L3, were each equipped with the ISCO 2105 Interface module (Teledyne ISCO) with a Ponsel Conductivity/Salinity sensor used to measure conductivity every 30 s, during the period from 20 March to 23 June. Calibration of the conductivity sensor was performed every second week using a conductivity standard (1413 µS) according to the manufacturer's recommendations.

Flow measurements

Flow measurements were performed at sampling stations A and E, using an ISCO 2150 Area Velocity module with a 15 s resolution. Because of some uncertainties in the measured data, detected during interim control of flow rate data, additional ISCO 2150 Area Velocity modules were installed in pumping stations P8A and P3A. Sensors of these additional modules were connected to anchors and mounted at the bottom of each pumping sump and used as sewage level meters. Logged time intervals between the water levels in the sump indicating the minimum and maximum values, together with the known dimensions of the sump, were also used for flow rate estimations.

All flow meter sensors were cleaned and calibrated weekly according to ISCO recommendations.

Flow velocity along the main sewer section

In order to estimate the velocity and time of travel of the flow in the main sewer section, dye testing was performed under dry weather conditions on 8, 9, and 15 June (1, 2 and 8 antecedent days, respectively). Every test started at 14:00 by introducing 100 mL of white dye at the upstream sampling station A. The time when the dye was clearly visible with peak intensity at the 17 selected manholes along the main sewer (including sampling stations A–E) was noted. Later, the flow velocity was calculated based on the distances among these 17 manholes.

Precipitation measurements

For rain measurements, a tipping bucket rain gauge (MJK Meteorological) was installed outside the building of the downstream pumping station P3A. The rain gauge had a collection area of 200 cm² and a resolution of 0.2 mm per bucket tip. Rain events in this study were considered to be independent events if there was at least a 3 h dry period between them.

Snow cover depth measurements were obtained from two stations of the Swedish Meteorological and Hydrological Institute (SMHI 2017) about 15 km away from the study area – see Panasiuk *et al.* (2019) for more details.

In total, 28 rainfall events with depths of 2 mm or more occurred during the study period between 20 March and 23 June. Fourteen of these had a rainfall depth of 5 mm or higher and are presented in Table 1.

RESULTS

Each method evaluated in this study identified a different number of I/I locations (actual or potential, as discussed further in the discussion section): DTS – 10 locations (seven during snowmelt and three during rain events); smoke testing – 15 locations (seven locations contributing during rain events or snowmelt, one misconnection of house drainage, and seven locations with smoke coming up through the soil); CCTV – 16 locations (ten locations with broken sewers, five inflows from the tributary sewers, and one direct inflow into the pipe); ammonium sampling by the automatic sampler – four

Table 1 | Summary of rain events during the monitoring campaign with a rain depth of 5 mm or higher

Event no.	Start		Duration (hh:min)	Rain depth (mm)	Average intensity (mm/h)
	Date	Time			
1	03-28	06:45	4:33	5.6	1.23
2	03-30	01:36	6:16	5.8	0.93
3	03-31	06:56	11:22	11.6	1.02
4	04-13	04:08	18:55	12.8	0.68
5	04-26	11:32	10:44	8.8	0.82
6	05-09	09:06	3:09	6.4	2.03
7	05-14	15:12	7:54	5.2	0.66
8	05-19	00:30	7:37	7.0	0.92
9	05-23	02:42	7:50	23.6	3.01
10	05-26	02:03	7:32	5.2	0.69
11	05-26	20:06	16:26	41.4	2.52
12	06-06	11:59	3:44	6.2	1.66
13	06-06	18:47	3:27	5.4	1.57
14	06-22	14:42	2:27	8.6	3.51

during snowmelt, three during rain events and one during dry weather; conductivity – one during snowmelt, five during rain events and one during dry weather; and, visual inspection – 47 locations (mostly as manhole covers located below the ground level and broken manholes, with only two locations with visible inflow from the manhole rings). For the grab sampling of ammonium, the decreases in concentration that might be caused by I/I were observed at 16 locations during upstream sampling and at 8–10 locations when sampling was carried out by following the flow travel (Lagrangian sampling).

DTS

The results of the DTS monitoring campaign in this study have been described in detail by Panasiuk *et al.* (2019). In short, the DTS analyses identified two separate groups of I/I locations: seven for snowmelt-induced I/I and three others for rainfall-induced I/I (Figure 1(a)). Locations for snowmelt-induced I/I identified by DTS were located around sampling station B, along the tributary sewer L1, and along tributary sewer L3. Rainfall-induced I/I was detected only after the most severe rain event during the study period (#11, depth=41.4 mm) and was located in the upstream section of the main sewer (Figure 1(a): $\delta 1$, $\zeta 3$, $\zeta 5$; Figure 2(d)) (Panasiuk *et al.* 2019).

CCTV

Based on the inspection protocols, 15 locations along the sewers were identified and classified as the following: ten cracked pipes (Figure 2(a)) or locations with root penetrations into sewers (Figure 2(b)), and five locations where visible inflow was coming from smaller tributary sewer connections into the main sewer section, and were interpreted by the CCTV inspector as I/I (Figure 1(a)). One additional location with relatively high I/I was found where a 3 m-long section of a concrete pipe had been installed between two PVC pipe sections (Figure 1(a), $\epsilon 8$).

The time of travel and flow velocity

Investigations of the time of travel, based on the dye testing performed on 8, 9 and 15 June, in dry weather conditions, showed the following results: on average, 53 ± 2.5 min were needed for the flow to travel from sampling station A to station B; 85 ± 1 min from A to C; 85.5 ± 1 min from A to D, and 108 ± 1 min from A to E (Figure 1(b)). The flow velocity reached its minimum of 0.2 m/s before stations C and D, and the maximum of 0.7 m/s at the downstream end of the main sewer section before station E (Figure 1(b)). The average flow velocity was estimated at 0.4 ± 0.1 m/s. Although the flow velocity may vary under different flow rate conditions, these estimated flow velocities and times of travel between the sampling stations were important when evaluating the results from the ammonium sampling by the automatic samplers, as any inflow at the upstream section would be detected in the samples collected at the downstream section 50 minutes later.

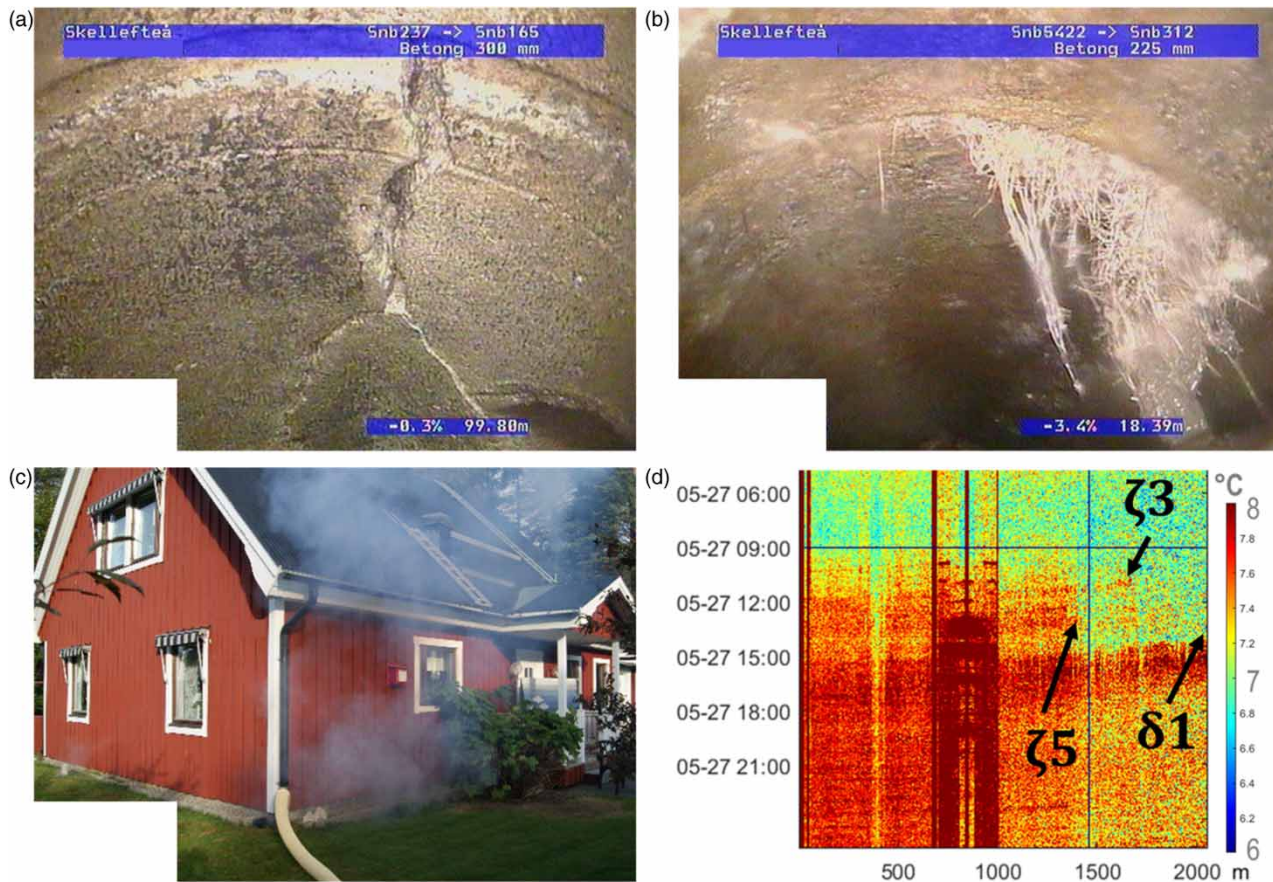


Figure 2 | Examples of the results found from (a) CCTV – cracked pipe; (b) CCTV – roots penetration; (c) smoke inspection – roof misconnection (for location, see Figure 1(a), $\epsilon 3$); (d) DTS – rain event #11 (for location, see Figure 1(a), $\delta 1$, $\zeta 3$, $\zeta 5$).

Ammonium concentrations

Ammonium sampling by automatic samplers

Snowmelt period. The results of the ammonium sampling by automatic samplers (presented in this section as the arithmetic mean \pm standard deviation) showed the following: in the course of the 24-hour sampling campaign, during the snowmelt period 16–17 April (Figure 3, top left), the average ammonium concentration at the upstream sampling station A was 6.2 ± 1.4 mg/L, with a local minimum of 3.7 mg/L at 07:00. At the next sampling station B, the ammonium concentration was 4.6 ± 0.8 mg/L, resulting in the largest decrease of 27% between stations A and B. The ammonium concentrations at stations C and D decreased by 12 and 4%, respectively. The only increase in mean ammonium concentration was found between stations C and D (from 4.0 ± 1.0 to 4.2 ± 0.5 mg/L); however, it was a statistically insignificant difference. In general, along the main sewer in the study section, the ammonium concentration decreased by 35% between the sampling stations A and E (from 6.2 ± 1.4 to 4.1 ± 0.6 mg/L) during the snowmelt sampling campaign period.

For the snowmelt period, the ammonium concentrations measured in the tributary sewers are presented in Figure 3, bottom left. The lowest ammonium concentrations were observed in tributary sewer L1 (0.74 ± 0.66 mg/L, with a minimum value of 0.08 mg/L), followed by L2 (3.2 ± 1.8 mg/L), and the highest concentrations were found in tributary sewer L3 (15 ± 6.5 , with a maximum of 28 mg/L).

During rain events. An example of the effect of rain events on ammonium concentrations in the sewers is presented in Figure 3 (top centre) showing a 48-hour sampling event on 25–27 May that covered rain event #10 (5.2 mm) and the most severe rain event #11 (41.4 mm). The ammonium values at the sampling stations along the main sewer section before rain

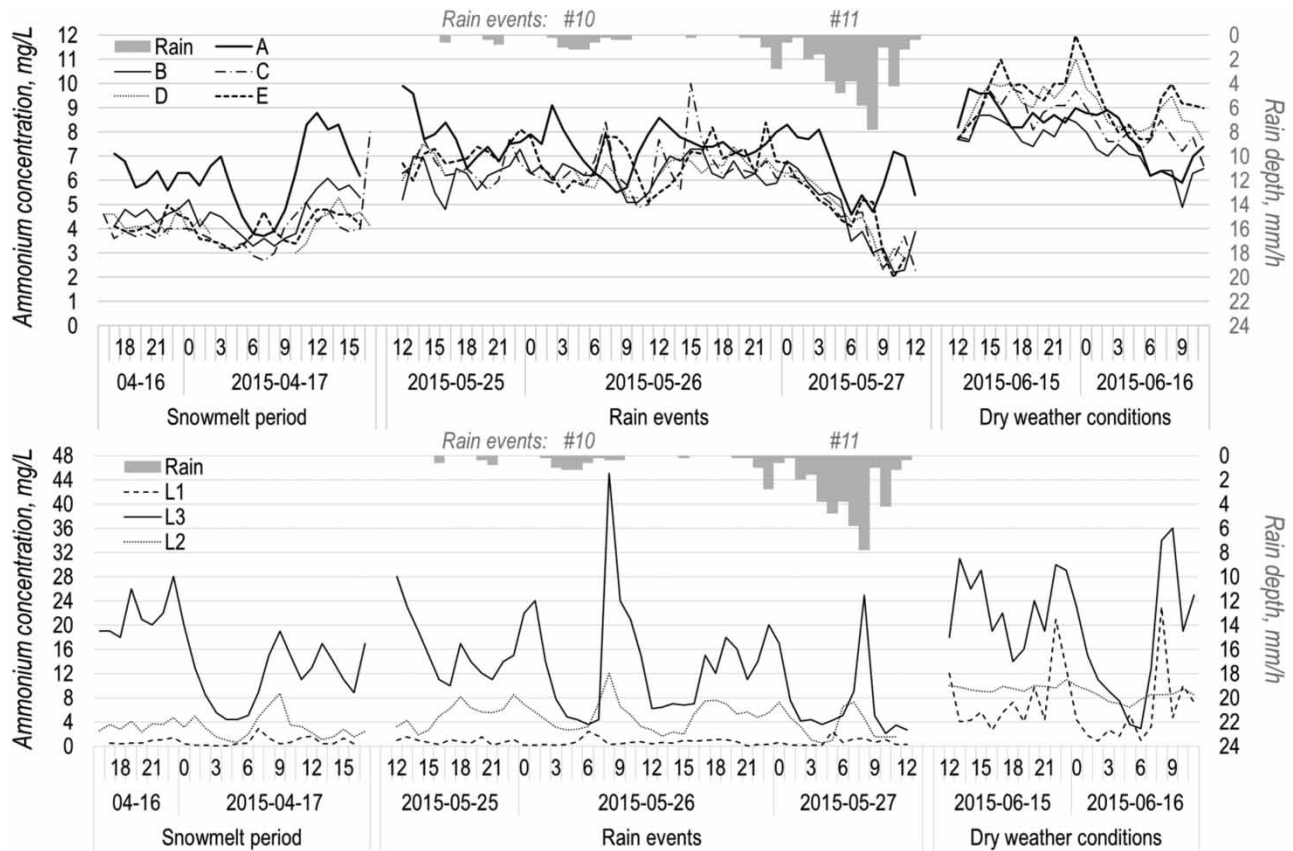


Figure 3 | Ammonium concentrations sampled by automatic samplers (left axis) and rain depth (right axis) along the main sewer section (top) and in tributary sewers (bottom) during the snowmelt period (left-hand section), rain events #10 and #11 (centre section) and dry weather conditions (right-hand section).

event #11 were slightly higher and statistically different from those measured during the snowmelt period: 7.5 ± 1.0 , 6.3 ± 0.7 , 6.6 ± 1.0 , 6.5 ± 0.6 and 6.8 ± 0.8 mg/L for the stations A–E, respectively. Several hours after the beginning of rain event #11, between 00:00 and 07:00 on 27 May, the ammonium concentrations at stations B–E reached the same level (standard deviation between four stations of 0.16–0.46 mg/L) and all four decreased from 6.5 ± 0.3 to 4.1 ± 0.4 mg/L. The ammonium concentration at station A responded to rain event #11 with a greater delay, compared to stations B–E: between 03:00 and 07:00, the concentration decreased from 8.3 to 4.6 mg/L. Between 07:00 and 09:00, there was some increase in ammonium concentrations, likely due to household water usage, up to 5.4 mg/L for station A and up to 4.6 ± 0.5 mg/L for stations B–E. For the period between 09:00 and 11:00, the concentration at station A increased to 7.2 mg/L, while concentrations at stations B–E continued to decrease, and at around 11:00 reached their minimum of 2.2, 2.8, 2.8 and 2.0 mg/L for stations B–E, respectively. The abovementioned decreases in ammonium concentration clearly indicated presence of I/I in the sewer system.

Ammonium concentrations in the tributary sewers L1 and L3 during rain events #10 and #11 (Figure 3, bottom centre) did not differ statistically from those obtained during the snowmelt sampling campaign: 0.71 ± 0.54 and 12 ± 8.4 mg/L, for the tributary sewers L1 and L3, respectively. A relatively high ammonium concentration of 45 mg/L was measured at 08:00 on 26 May, after rain event #10 and before the biggest rain event, #11, for inflow L3. However, the ammonium concentration in the tributary sewer L2 during the rain sampling campaign was higher and significantly different (4.7 ± 2.4 mg/L, Figure 3, bottom centre) from the snowmelt sampling campaign. This indicates that in tributary sewer L2, less I/I ingress was caused by rain than snowmelt. Decreases in ammonium concentrations during rain events #10 and #11 were observed in all tributary sewers, although it was difficult to conclude whether those decreases were caused by daily variations of ammonium in the wastewater or by I/I.

Dry weather conditions. The 24-h sampling campaign during dry weather conditions on 15–16 June (Figure 3, right) showed significantly higher ammonium concentrations compared to those during the snowmelt and rain event sampling campaigns at all sampling stations along the main sewer section. Another important distinction between the dry weather sampling and the two other sampling periods was that the ammonium concentration in general increased along the main sewer section (apart from the section between stations A and B): 8.1 ± 1.1 , 7.4 ± 1.0 , 8.4 ± 0.9 , 9.1 ± 0.9 and 9.4 ± 1.1 mg/L for stations A–E, respectively (Figure 3, top right), with a 15% increase on average between stations A and E. These findings indicated increased contributions of household wastewater, compared to the I/I fraction in sewers, during dry weather conditions.

A statistically significant difference in ammonium concentrations between the dry weather and the two wet weather sampling campaigns was also observed in tributary sewers L1 and L2, with average concentrations for dry weather sampling of 6.6 ± 5.8 and 9.0 ± 1.1 mg/L, respectively (Figure 3, bottom right). For tributary sewer L1, the ammonium concentration was 9.0 times higher than the average concentrations during snowmelt and 9.4 times higher than during rain event campaigns. No significant difference was found between the dry (19.8 ± 9.3 mg/L) and snowmelt sampling campaigns in tributary sewer L3.

Upstream grab sampling for ammonium analyses

Grab samples collected during the dry weather conditions on 29 April in both the main sewer section (Figure 1(c)) and some tributary sewers (bold numbers in Figure 1(a)) produced the results presented below. At the upstream end of the main sewer section, the ammonium concentration was 8.5–8.8 mg/L. From that point, the ammonium concentration decreased along the sewer, with the largest decrease around sampling station B, down to 5.0 mg/L. The ammonium concentration varied between 4.0 and 4.9 mg/L in the village centre and then increased to 5.0–5.8 mg/L towards the downstream end of the main sewer section, likely due to increased contribution of wastewater from the households in that area (Figure 1(c)). Low concentrations of ammonium were measured in three smaller tributary sewers in the upstream half of the study section (9.0 ± 0.20 , 4.0 ± 0.93 and 0.9 ± 0.09 mg/L), as well as inside tributary sewer L5 (3.0 ± 0.06 mg/L) (see Figure 1(a), $\epsilon 2$, $\epsilon 9$, $\epsilon 14$ and $\delta 8$, respectively). Such low concentrations of ammonium could indicate the presence of I/I in these four tributary sewers. In contrast, samples taken in tributary sewers L3 and L4 (Figure 1(a), $\gamma 12$) had relatively high ammonium concentrations, 34.7 ± 0.58 and 49.7 ± 1.53 mg/L, respectively, indicating low I/I presence in these two pipes. No samples were collected from L2 on 29 April.

Lagrangian sampling for ammonium analyses following the flow through the study section

The grab sampling along the flow was performed on 8, 9 and 15 June, in dry weather conditions and at the same starting time of 14:00. The ammonium concentrations along the sewer in the samples taken on 8 and 9 June showed a statistically insignificant decrease around station B (from 8.0 and 8.4 to 7.1 and 7.5 mg/L, respectively), which was also observed in the upstream sampling campaign, possibly due to the I/I contribution from tributary sewer L1. In agreement with the upstream sampling results, on 9 and 15 June, the concentrations of ammonium increased (statistically significantly) after passing by the village centre (stations C/D, from 7.2 and 7.1 to 8.3 and 8.5 mg/L, respectively), likely due to an increased share of contribution of household wastewater (Figure 1(d)).

In general, the ammonium concentrations detected during the three Lagrangian sampling events that followed the flow showed less variation as compared to the upstream sampling. This could be explained by the fact that not only I/I but also the diurnal variations in ammonium discharge to the sewers might have influenced the results in the upstream sampling (Figure 1(c) and 1(d)).

Flow measurements

Initially, in order to measure the flow rates at the upstream and downstream ends of the study section, ISCO flowmeters were installed at pumping stations P8A and P3A. However, even with regular (roughly every week) cleaning and level calibration, these flow meters produced unreliable results. Therefore, an additional flow measurement technique was applied, namely, measuring the time it took for the sewer flow to fill up a known volume in the sumps of the pumping stations. This method provided some flow rate information, but proved to have limitations in terms of accuracy and ability to measure high flows above the pump capacity of about 24 L/s.

Conductivity

The results of the conductivity measurements showed clear daily variations in the main sewer section (Figure 4, top). During the snowmelt period, the peaks occurred around 14:00–16:00 and troughs around 07:00–09:00, while during rainy and dry

weather conditions, the peaks shifted to around 22:00–02:00 and troughs to around 10:00–14:00 (Figure 4, top). Tributary sewers had a similar, but sometimes less obvious, daily pattern (Figure 4, bottom). The conductivity in tributary sewers (except L1 during snowmelt and rain event periods) had higher fluctuations compared to those in the main sewer section, likely due to higher variations in wastewater fraction from households.

During the snowmelt period, the conductivity at the upstream end of the main sewer section (station A) was $209 \pm 20 \mu\text{S}/\text{cm}$ and decreased significantly at the next downstream station B to $143 \pm 21 \mu\text{S}/\text{cm}$, likely due to I/I. Further downstream in the main sewer pipe, the conductivity increased to $173 \pm 11 \mu\text{S}/\text{cm}$ at station C and to $184 \pm 11 \mu\text{S}/\text{cm}$ at station E, likely due to increased inflows of wastewater from households in the area (Figure 4, top left). No data were available at station D, because of logger malfunction. Conductivity at tributary sewer L1 was relatively stable, around $154 \pm 8 \mu\text{S}/\text{cm}$, while at station L3 it fluctuated from 129 to $482 \mu\text{S}/\text{cm}$ (269 ± 84) (Figure 4, bottom left). Data for station L2 were missing, because of logger malfunction.

Overall, during the snowmelt period, the conductivity at station E was lower than at station A, indicating strong influence of I/I on the main sewer section. These differences were maximal from around 15:00–03:00 and almost disappeared completely between 08:00 and 11:00, which could be explained by two factors: daily patterns of wastewater inflow to the sewers increasing the conductivity, and snowmelt-induced I/I decreasing the conductivity. For the latter, the daily temperature variations driving snowmelt intensity were found to be mimicked by the variations and differences in conductivity between stations A and E, with a 4–6 hours delay. During two nights, on 18 and 20 April, the temperature was below 0°C and, therefore,

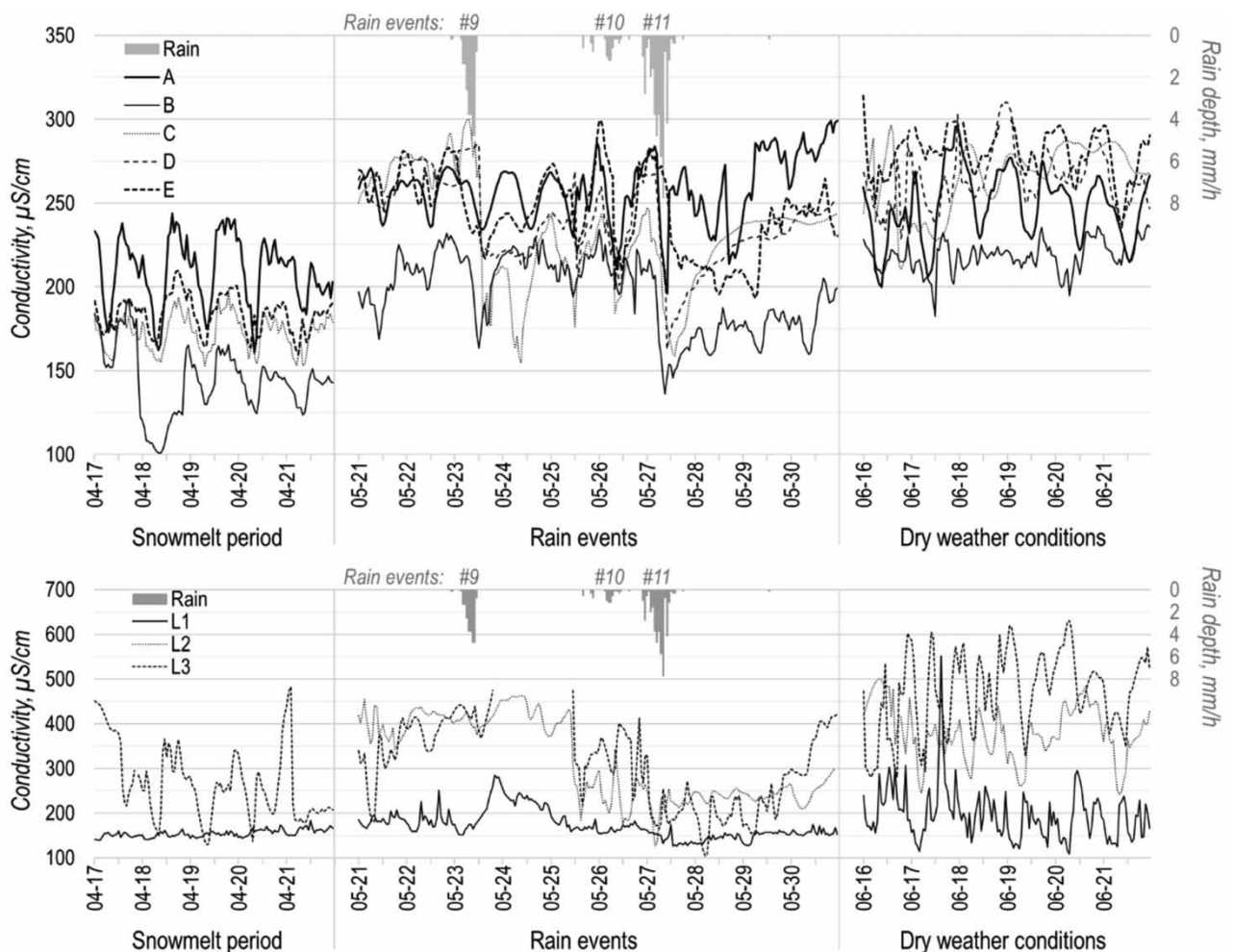


Figure 4 | Conductivity measurements (left axis) and rain depth (right axis) along the main sewer section (top) and from tributary sewers (bottom) during the snowmelt period (left-hand section), rain events #9, #10 and #11 (centre section) and dry weather conditions (right-hand section). Note the difference in the left y-axis between top and bottom panels.

no snowmelt occurred. These nights were the only two occasions during the snowmelt period with higher conductivity measured at the downstream end of the main sewer section, compared to the upstream end.

All three rain events #9, #10 and #11 presented in Figure 4 (centre) occurred at the times of daily troughs in conductivity variations (from around 10:00 until 14:00); therefore, conductivity patterns before rain event #9 were used for the analysis of I/I influence.

Prior to rain event #9, conductivities at stations A, C, D and E were nearly equal with low fluctuations (average for 45 hours: 258 ± 10 , 270 ± 9 , 264 ± 10 and 263 ± 11 $\mu\text{S}/\text{cm}$, respectively), and were significantly higher than conductivity at station B (206 ± 15 $\mu\text{S}/\text{cm}$). At stations L1, L2 and L3, conductivity was around 183 ± 17 , 348 ± 32 and 403 ± 29 $\mu\text{S}/\text{cm}$, respectively. All of these measured values for both the main sewer section and tributary sewers were significantly higher compared to those collected during the snowmelt period, indicating less I/I prior to rain event #9, compared to the snowmelt period. Lower concentrations measured at station B might indicate a higher proportion of I/I in the sewers between stations A and B, as well as in the tributary sewer L1 as indicated by the measurements.

After rain event #9 had finished, a significant drop in conductivities was observed at station C, followed by stations D, B and E (Figure 4, top centre). The conductivity of the wastewater at the upstream station A, as well as at all three tributary sewers L1, L2 and L3, seemed to be unaffected by rain event #9 (Figure 4, centre). After about 24 hours, conductivity at the downstream end of the main sewer section returned to the same level as at the upstream end. During rain event #10, the only stations that showed a clear decrease in conductivity were A and E. Finally, rain event #11 caused a significant decrease (around 90 $\mu\text{S}/\text{cm}$ on average) in conductivity for all stations (except, possibly, station L1). In general, conductivity at the downstream end (station E) of the main sewer was 39 ± 17 $\mu\text{S}/\text{cm}$ lower than at the upstream end (station A) after rain event #11 (Figure 4, top centre), and this difference was statistically significant. The decreases in conductivity during these rain events could be explained by rain-induced I/I entering the wastewater sewer.

During the dry weather conditions in June, the average conductivity levels at each station (A–E) were statistically significantly higher than during the snowmelt (Figure 4, right). At the upstream end of the main sewer section, station A, conductivity was 248 ± 21 $\mu\text{S}/\text{cm}$. At the following station B, the conductivity was lower, 218 ± 9 $\mu\text{S}/\text{cm}$, which could be explained partly by water with low conductivity coming from tributary sewer L1, 195 ± 58 $\mu\text{S}/\text{cm}$. Further downstream of station B, the conductivity along the main sewer section not only increased but exceeded the values at upstream station A. At station C and at its tributary sewer L3, conductivity was 266 ± 20 and 471 ± 90 $\mu\text{S}/\text{cm}$, respectively. At station D and at its inflow L2, the corresponding values were 265 ± 18 and 380 ± 62 $\mu\text{S}/\text{cm}$, respectively, while at downstream station E conductivity was 279 ± 14 $\mu\text{S}/\text{cm}$. All of the abovementioned differences in conductivity among sampling stations A–E were statistically significant, except for the difference between stations C and D. The fact that conductivity at downstream station E was higher than at station A only during dry weather conditions suggests that the I/I impacts were considerably reduced, compared to those during the snowmelt and rain events.

Statistically significant decreases were found between the conductivity levels before and after rain events #9–11 at the most downstream sampling station E, as well as between stations A and E after the rains. However, no statistically significant differences were observed before and after rains #9–11 at sampling station A or between station A and E before rain events #9–11. It was, therefore, concluded that most of the rain-induced I/I was entering the sewers within the study area, rather than via the sewers located upstream.

Smoke and dye test inspections

The smoke and dye test inspection company identified six roofs (Figure 2(c)) (marked with triangles in Figure 1(a), $\delta 2$, $\epsilon 2$, $\epsilon 3$, $\zeta 7$, $\delta 12$, $\delta 12$), one gully pot in front of a garage door (Figure 1(a), $\delta 2$), and one basement drain (Figure 1(a), $\delta 14$) that were misconnected to the sanitary sewers. Additionally, seven locations were detected where smoke was coming up from the ground during the inspection (Figure 1(a), $\zeta 6$, $\zeta 8$, $\beta 14$, $\beta 14$, $\alpha 15$, $\alpha 15$, $\delta 14$).

Manhole inspections and photos

Both the municipality and the smoke testing company made visual inspections of the condition of manholes (Figure 1(a)). The identified problems were divided into four categories: (a) 32 manhole covers in depressions below the ground level, (b) five broken manhole covers, (c) eight broken manholes structures or manholes with root penetrations, and (d) two instances of visible inflow of I/I into the manholes (Figure 1(a), $\epsilon 1$, $\epsilon 2$). The first three categories did not directly indicate I/I, but rather an increased risk of I/I under certain conditions.

DISCUSSION

Identification of I/I

In order to remove sources of I/I in the sewer system, the associated ingresses of extraneous water need to be identified and localised (Schilperoort *et al.* 2013).

One way of comparing the performance of the evaluated methods in I/I identification, i.e., confirming the presence of I/I in sewers, is to compare the number of I/I locations detected by the methods tested. Theoretically, the methods that reliably detect more I/I locations in the same study section perform better in I/I identification. However, such a mechanical approach to the method evaluation does not account for differences in accuracy, temporal and spatial resolution (as discussed in the forthcoming sections), the length of the sewers monitored, or whether the detected locations actually contribute to I/I, or merely have the potential to do so. It was decided to exclude some of the detected locations that were considered as false positive results as discussed below.

Some problematic cases, such as broken manhole covers or root penetrations into sewers, are just indications of risk of I/I under certain conditions (Field & O'Connor 1997; Stauffer *et al.* 2012). However, in the present study, such cases did not contribute any visible direct inflows of extraneous water that would be detected by the other methods evaluated. Excluding such locations from method comparisons reduced the number of detected locations from 16 to six for CCTV and from 47 to just two for visual inspections. Misconnected roofs and gully pots (eight locations) did not contribute to I/I during the periods of smoke testing; however, these locations would most definitely generate I/I during rain events (Rödel *et al.* 2017) and were, therefore, included in the comparisons. Seven locations with smoke coming up from the ground were excluded from the comparison for smoke testing. For the ammonium and conductivity tracing, the number of I/I identifications was considered as the number of decreases in measured values either between two sampling stations (for snowmelt and dry weather periods) or at the individual sampling stations (for the rain events). Such decreases were almost all statistically insignificant, when two adjacent sampling locations were compared: 15 out of 16 decreases for the manual ammonium sampling and seven out of eight decreases in ammonium concentration sampling following the flow. Another issue is the frequency of sampling and daily variations in ammonium concentration, which is discussed at the end of this section. In practice, however, low ammonium concentration at any sampling site is by itself an indication of the presence of I/I in the sewer system. For example, Uusijärvi (2013) used ammonium concentrations below 20 mg/L as indicators of the presence of I/I.

Out of six I/I locations identified by CCTV, one contributed considerable inflow of groundwater from the surrounding soils to the sewer, at a location where a 3 m-long concrete pipe was unexpectedly found joining two PVC pipe sections (Figure 1(a), $\epsilon 8$). The other five locations classified as inflow of water from smaller tributary sewers showed relatively clear water flowing into the inspected sewers on video. A number of studies have shown CCTV surveys to be a subjective method that relies on the visual interpretations of the CCTV inspector (Pitt 2004; Panasiuk *et al.* 2015), and as such, might not reliably distinguish I/I from some types of households wastewater inflows with low particle content.

Therefore, concerning the identification of I&I sources, it was concluded that the DTS method identified ten I/I locations and smoke testing eight locations. The other methods reliably detected only one or two I/I locations.

Accuracy

For each method, the accuracy of I/I detections was evaluated by assessing whether or not other methods identified I/I at the same locations. If several methods detected I/I in the same location, this increases their accuracy or 'trueness' in terms of International Organization for Standardization (ISO) 5725-1. Such an approach supports the minimisation of the number of false positive detections for some methods as discussed in the previous section. However, it is worth noting that not all methods can be 'proved' by another method, especially if the monitoring campaign is relatively short. For example, smoke inspection provides evidence of a misconnected roof that cannot be found by another method until it rains. Another example is DTS, which may detect a short rain event that was missed by CCTV or grab sampling of ammonium that happened before or after the rain event.

At the upstream end of the study section, the DTS, ammonium and conductivity methods detected I/I during the rain event #11 (Figure 1(a), $\delta 1$). Downstream of station A, both the CCTV and the visual inspection found a visible inflow from a tributary sewer ($\epsilon 2$). Then, inflow from one misconnected roof was confirmed by DTS during rain event #11 and also by smoke testing ($\zeta 3$). At four different locations, between stations A and B, both the CCTV and ammonium grab sampling indicated the presence of I/I ($\zeta 3$, $\zeta 4$, $\zeta 5$, $\zeta 7$). Additionally, CCTV and smoke inspection indicated I/I at the same location ($\zeta 6$). Upstream of

station B, the CCTV, smoke testing, DTS, conductivity, and automatic and grab sampling of ammonium detected I/I ($\zeta 8$). Along tributary sewer L1, both DTS and CCTV detected I/I during snowmelt ($\epsilon 8$). A misconnected house drain at the downstream end of the sewers was detected by smoke inspection and ammonium grab sampling, contributing flow on 15 June (see Figure 1(a), $\delta 14$).

In rainy weather during the study period, DTS did not detect two misconnected roofs and one gully pot in the eastern part of the study section (Figure 1(a), $\delta 2$, $\delta 2$, $\epsilon 2$), one roof in the middle part ($\zeta 7$), and two roofs draining to tributary sewer L2 ($\delta 12$, $\delta 12$); all six were detected by smoke testing. A study by Nienhuis *et al.* (2013) focusing on the detection limits of DTS showed that even for larger volumes of inflow, the temperature response of DTS cables was reduced by more than 50% due to the energy losses in 8-m long tributary sewers, when compared to direct inflow (i.e., a zero length pipe). In this study, water from the misconnected gully pot and roofs had to travel 120–160 m through the tributary sewer before reaching the main sewer with the DTS cable. Therefore, it is improbable that there would be any detectable temperature differences, attributable to the aforementioned inflows, in the DTS temperature plots for the main pipe.

Location: temporal and spatial resolution

Since successful identification of I/I depends to a great extent on how frequently a method can provide readings from the same location and how accurately it can localise I/I, the temporal and spatial resolution of the studied methods were investigated.

Among the evaluated methods, the online methods (DTS, conductivity and flow measurements) were the ones with the highest time resolution (30 s, or less). CCTV and visual inspections cannot, in this sense, be considered online methods even if applied over some time duration at one location, since they serve to produce momentary measurements at different locations in the sewer network. These two methods are often used as a part of municipal I/I campaigns (with a service cycle of around 10–20 years), during daytime and dry weather conditions, limiting their suitability for detection of I/I caused by rainfall runoff (Panasiuk *et al.* 2015). This makes both CCTV and visual inspection less efficient in identification of shorter-duration inflows caused by rainfall runoff than of other types of I/I (groundwater infiltration and snowmelt-induced runoff inflow).

Automatic samplers used to collect samples for ammonium analyses usually allow flexibility concerning the time resolution, with sampling intervals as short as 1 min, depending on the selected length of sampling and frequency of maintenance (Galfi *et al.* 2014; Mattsson *et al.* 2016). The selected sampling frequency also affects the results due to ammonium variations in wastewater, as discussed in the section below.

As for locating the sources of I/I, the abovementioned methods varied in their spatial resolution, from providing an exact position (± 0.5 m, by DTS, sometimes smoke testing and CCTV inspections) (Hoes *et al.* 2009) and pinpointing specific tributary sewers (CCTV, sometimes visual inspections) (Butler & Davies 2010), to identifying the sewer sections between two manholes (ammonium grab sampling, visual inspection) (Irvine *et al.* 2011), or between two sampling stations (conductivity, ammonium automatic samplers) (Schilperoort *et al.* 2006; Irvine *et al.* 2011), or two pumping stations (flow measurements). Flow measurements at one upstream and one downstream pumping station have a spatial resolution of the upstream contributing catchment. However, such a resolution could be increased by adding more flow meters at intermittent locations.

Volume estimation

Most of the methods evaluated in this study (flow measurements, ammonium concentration, conductivity, DTS) require accurate flow measurements for estimating I/I volumes. However, even with a proper installation layout and regular maintenance of flowmeters, considered as the two most important factors affecting flow measurement accuracy (Campisano *et al.* 2013), three different flow measurement methods applied in this study proved to be rather tedious and produced results with large uncertainties. Consequently, volume estimations were excluded from this paper. Flow measurement issues also prevented taking full advantage of Lagrangian sampling by testing quantitative flow mass analysis.

Frequency and uncertainty of ammonium sampling

In order to evaluate the influence of ammonium sampling frequency on the obtained results, ammonium sampling by the automatic sampler was performed every 5 min for 2 hours during the day (13:00–15:00, on 16 June) and at night (03:00–05:00, on 17 June) at the downstream sampling station E during dry weather conditions (Figure 5).

Firstly, applying the same procedure as described in the Materials and methods section to obtain 1 h time-weighted ammonium concentration values from four 15 min subsamples (Figure 5, X-markers), the ammonium concentrations would be 8.7 and 8.6 mg/L during the day and 8.9 mg/L for both hours at night (Figure 5, dashed line). If the sampling was delayed for 5 min (Figure 5, O-markers), the same procedure would result in different averages: 9.5 and 8.9 mg/L during the day, and 9.0 and 8.5 mg/L at night (Figure 5, dotted line), i.e. a difference from -4.5% to $+9.2\%$ in comparison to the original sampling (Figure 5, X-markers).

Secondly, the results showed that the ammonium concentration varied between 7.9 and 10.0 mg/L during the day and between 7.1 and 9.5 mg/L during the night for the 5-min samples. If compared to the average hourly sample concentrations of 12 5-min subsamples, taking one sample per hour generates a difference of between -19.3% and $+14.9\%$, and between -8.5% and $+6.1\%$ for two samples per hour.

A number of studies, including two reports from the Swedish Water & Wastewater Association (Lundblad & Backö 2012; Uusjärvi 2013; Zhang *et al.* 2018a), have suggested ammonium concentration as a promising indicator of I/I; however, their methodologies suggest taking a single sample per location (Zhang *et al.* (2018a) took one sample every 2 hours). Such approaches increase uncertainty in the interpretation of results of ammonium sampling and estimation of I/I in sewers as compared to either more frequent sampling or composite sampling as discussed above.

Ammonium sampling strategies

Three ammonium sampling strategies were used in this study: automated sampling, upstream grab sampling, and grab sampling following the flow. Each of these presented some advantages and practical limitations, as discussed below.

Automatic or grab sampling?

The chief advantage of automatic sampling was its ability to take a number of samples (24–48 in this study) during a period of time (1–2 days). This makes automatic sampling more suitable for covering short-term I/I events (e.g., short rains or intensive snowmelt). In addition, it is possible to program multiple automatic samplers to take samples simultaneously at several locations (Panasiuk *et al.* 2016). With some practice and planning, it was possible to run eight samplers over a 2-day sampling period by only one person in this study.

The most important limitation of automatic ammonium samplers is that this method usually requires a stationary sampling station that cannot be moved easily to another location if needed, while grab samples could be collected at any available man-hole. Another difference between the two sampling methods is that an automatic sampler involves lower operational costs but higher initial investment, while grab sampling requires additional personnel for each simultaneous sampling. Finally, the issues of practicality and field safety can make one or another method suitable for specific sampling conditions (Galfi *et al.* 2014).

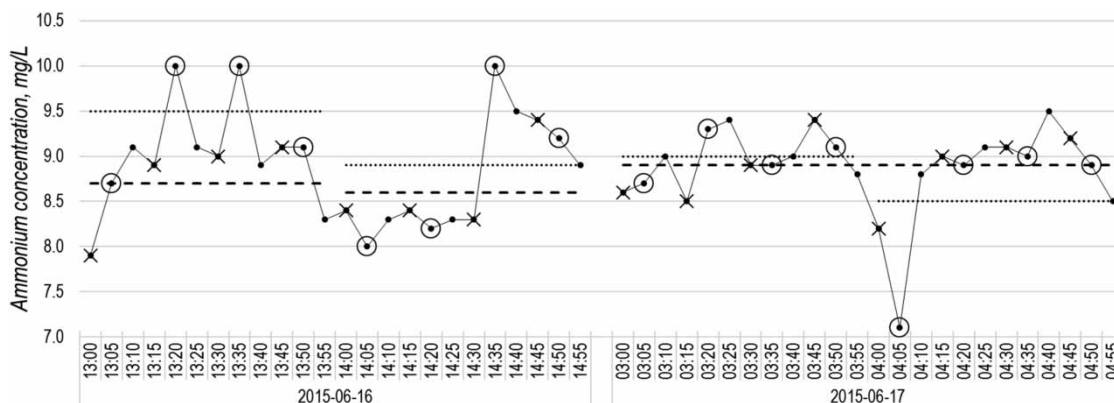


Figure 5 | Ammonium concentrations in samples collected by the automatic sampler every 5 minutes during the daytime (left) and at night (right) at sampling station E. X- and O-markers indicate subsamples that would be taken during regular 15 min time-weighted sampling and same sampling with 5 min delay, respectively. Dashed and dotted lines show resulting average hourly sample concentrations for regular and delayed sampling, respectively.

Upstream grab sampling or Lagrangian sampling following the flow?

Upstream grab sampling has mainly been used as a source location method, moving upstream from a location where low concentration of ammonium was detected (e.g. less than 20 mg/L) until a concentration above threshold was measured (Uusijärvi 2013). Initially, sampling only at downstream locations provided fast screening of sub-catchments, while moving upstream localises I/I with the desired spatial resolution (up to a distance between two adjacent manholes). An additional advantage of this approach is that tributary sewers in the catchment can be sampled if needed.

In practice, Lagrangian ammonium sampling following the flow requires more planning (e.g. concerning which manholes to sample, time needed per sampling location, and time needed to travel to the next location) as compared to upstream grab sampling. Due to the limited time window for each location, no additional samples from tributary sewers could be taken using ammonium sampling following the flow.

Both of the evaluated grab sampling methods allowed estimation of I/I fraction provided that a reference value for ammonium concentration was available (e.g. 40 mg/L) (Mattsson *et al.* 2016). A major limitation of the upstream grab sampling method is that it does not take into consideration diurnal and day-of-the-week variations of ammonium concentration in wastewater flow. Measurements performed at a similarly sized catchment in southern Sweden on four occasions between May 2006 and May 2007 showed variation in ammonium concentration between 34 and 53 mg/L (Gryaab 2008). The chief advantage of Lagrangian ammonium grab sampling following the flow was that it minimised the influence of the diurnal variation of ammonium, so any changes in measured concentration could be related to the increased or decreased effect of I/I.

CONCLUSIONS

The methods studied in this paper have shown varied performance with respect to identification and location of I/I sources, and differ in accuracy and in temporal and spatial resolutions. Depending on the main focus of an I/I monitoring programme, a combination of two to three methods may be used in order to improve the efficiency of such programmes. For example, flow measurements at pumping stations (a city level), ammonium grab sampling (prioritising sewer sections) and DTS (identifying accurate location) may be used in an I/I location and elimination programme.

In this study, DTS monitoring proved effective in identification of I/I during both the snowmelt period and rain events, identifying ten I/I locations, followed by smoke testing with eight identified I/I locations. Methods based on ammonium concentrations (using an automatic sampler) and conductivity measurements were limited to the locations of the sampling stations. Grab sampling of ammonium both upstream and following the flow indicated 16 I/I locations by decrease in measured concentrations; however, most such decreases (15 out of 16) were found to be statistically insignificant. Only one out of six I/I locations identified by CCTV could be confirmed as I/I, while the other five locations had relatively clear water coming from tributary sewers that might be difficult to distinguish reliably from some types of household wastewater.

Methods with a higher spatial resolution (DTS, smoke testing, and CCTV) were able to pinpoint I/I locations with an accuracy of some decimetres. This can be especially important for I/I monitoring campaigns in sewers with many tributary sewers and for avoiding too much excavation if a pipe has to be replaced. From another perspective, low spatial resolution methods (e.g. ammonium sampling and conductivity measurements) have been shown to be efficient for the initial screening of larger catchments.

Methods with a higher time resolution (e.g., online methods like DTS and conductivity) are able to capture rapid changes caused by I/I, increasing the probability of detecting the effects of short-duration rain events, as compared to low-time resolution methods like automated ammonium sampling. In this study, ammonium sampling by an automatic sampler was applied during a relatively long rain event (more than 16 hours) and, therefore, was also able to detect rain-caused I/I. Sampling with a higher time resolution (5 min) provided information about the variability of ammonium concentrations and reduced the uncertainty in low resolution (1 h) sampling results (ammonium concentrations) from 34.2% to 13.7%.

The initially planned comparison of methods of I/I volume estimation was excluded from this study as flow measurements proved to be onerous in producing reliable data. In order to produce reliable direct flow measurements, more maintenance or other types of flow measuring techniques than used in this study (e.g., no-contact flow meters) are required.

Three methods of ammonium sampling showed advantages and limitations. Automatic samplers are best suited to detect short-duration I/I episodes caused by rain or intensive snowmelt; several samplers can be programmed to collect samples

simultaneously, but their locations are fixed by the locations of sampling stations. Upstream grab sampling at localised sections of sewers with suspected I/I allowed for adjustment of the spatial resolution by collecting more or fewer samples and sampling in tributary sewers. Upstream grab sampling entails a higher degree of uncertainty, as compared to grab sampling following the flow due to daily variations of ammonium concentrations. In turn, Lagrangian sampling following the flow requires significant preparations (i.e., acquiring a sewer plan; planning, which manholes to sample; finding those manholes in the terrain; and ensuring that those manholes can be safely opened and closed, etc.), and usually only the main sewer section can be sampled, because of limited time between sequential samples.

DTS monitoring showed different locations for I/I during snowmelt period and during rain events, suggesting different pathways for I/I. Performing I/I monitoring during and after snowmelt is therefore recommended for I/I monitoring campaigns in cold climates. Among the selected methods, visual (photo) inspection provided the least amount of information in terms of identification, location or volume estimation of I/I. It is therefore recommended to perform visual inspection only as a part of another type of investigation (e.g. CCTV).

DATA AVAILABILITY STATEMENT

All relevant data are included in the paper or its Supplementary Information.

REFERENCES

- Barber, L. B., Antweiler, R. C., Flynn, J. L., Keefe, S. H., Kolpin, D. W., Roth, D. A., Schnoebelen, D. J., Taylor, H. E. & Verplanck, P. L. 2011 Lagrangian mass-flow investigations of inorganic contaminants in wastewater-impacted streams. *Environ. Sci. Technol.* **45**, 2575–2583. <https://doi.org/10.1021/es104138y>.
- Beheshti, M. & Sægrov, S. 2019 Detection of extraneous water ingress into the sewer system using tandem methods – a case study in Trondheim city. *Water Sci. Technol.* **79** (2), 231–239.
- Butler, D. & Davies, J. 2010 *Urban Drainage*, 3rd edn. CRC Press, London.
- Cahoon, L. B. & Hanke, M. H. 2017 Rainfall effects on inflow and infiltration in wastewater treatment systems in a coastal plain region. *Water Sci. Technol.* **75**, 1909–1921. <https://doi.org/10.2166/wst.2017.072>.
- Campisano, A., Ple, J. C., Muschalla, D., Pleau, M. & Vanrolleghem, P. A. 2013 Potential and limitations of modern equipment for real time control of urban wastewater systems. *Urban Water J.* **10**, 300–311. <https://doi.org/10.1080/1573062X.2013.763996>.
- De Bénédictis, J. & Bertrand-Krajewski, J. L. 2005 Infiltration in sewer systems: comparison of measurement methods. *Water Sci. Technol.* **52**, 219–227.
- Field, R. & O'Connor, T. P. 1997 Control strategy for storm-generated sanitary-sewer overflows. *J. Environ. Eng.* **123**, 41–46.
- Galfi, H., Nordqvist, K., Sundelin, M., Blecken, G.-T., Marsalek, J. & Viklander, M. 2014 Comparison of indicator bacteria concentrations obtained by automated and manual sampling of urban storm-water runoff. *Water, Air, Soil Pollut.* **225**, 1–12. <https://doi.org/10.1007/s11270-014-2065-z>.
- Gryaab 2008 Provtagningar i referensområden 2006/2007, Hushållsspillvatten Del 1 (Sampling in reference areas 2006/2007, Domestic wastewater Part 1) (No. 2008:6).
- Hoes, O. A. C., Schilperoort, R. P. S., Luxemburg, W. M. J., Clemens, F. H. L. R. & van de Giesen, N. C. 2009 Locating illicit connections in storm water sewers using fiber-optic distributed temperature sensing. *Water Res.* **43**, 5187–5197. <https://doi.org/10.1016/j.watres.2009.08.020>.
- International Organization for Standardization ISO 5725-1. 1994 Accuracy (trueness and precision) of measurement methods and results – part 1: general principles and definitions ISO, Geneva, pp. 1-17
- Irvine, K., Rossi, M. C., Vermette, S., Bakert, J. & Kleinfelder, K. 2011 Illicit discharge detection and elimination: low cost options for source identification and trackdown in stormwater systems. *Urban Water J.* **8**, 379–395. <https://doi.org/10.1080/1573062X.2011.630095>.
- Karpf, C. & Krebs, P. 2011 Quantification of groundwater infiltration and surface water inflows in urban sewer networks based on a multiple model approach. *Water Res.* **45**, 3129–3136. <https://doi.org/10.1016/j.watres.2011.03.022>.
- Lundblad, U. & Backö, J. 2012 *Undersökningsmetoder för att hitta källorna till tillskottsvatten (Survey Methods to Find the Sources of Infiltration and Inflow)* (No. 2012–13), *Svenskt Vatten Utveckling*.
- Mattsson, J., Mattsson, A., Davidsson, F., Hedström, A., Österlund, H. & Viklander, M. 2016 Normalization of wastewater quality to estimate infiltration/inflow and mass flows of metals. *J. Environ. Eng.* **142**. [https://doi.org/10.1061/\(ASCE\)EE.1943-7870.0001120](https://doi.org/10.1061/(ASCE)EE.1943-7870.0001120)
- Nienhuis, J., De Haan, C., Langeveld, J., Klootwijk, M. & Clemens, F. 2013 Assessment of detection limits of fiber-optic distributed temperature sensing for detection of illicit connections. *Water Sci. Technol.* **67**, 2712–2718. <https://doi.org/10.2166/wst.2013.176>.
- Panasiuk, O., Hedström, A., Marsalek, J., Ashley, R. M. & Viklander, M. 2015 Contamination of stormwater by wastewater: a review of detection methods. *J. Environ. Manage.* **152**, 241–250. <https://doi.org/10.1016/j.jenvman.2015.01.050>.
- Panasiuk, O., Hedström, A., Ashley, R. M. & Viklander, M. 2016 Detection of wastewater discharges into stormwater sewers: effects of travel distance on parameters. *J. Environ. Eng.* **142**, 04016016. [https://doi.org/10.1061/\(ASCE\)EE.1943-7870.0001086](https://doi.org/10.1061/(ASCE)EE.1943-7870.0001086).

- Panasiuk, O., Hedström, A., Langeveld, J., de Haan, C., Liefing, E., Schilperoot, R. & Viklander, M. 2019 Using distributed temperature sensing (DTS) for locating and characterising infiltration and inflow into foul sewers before, during and after snowmelt period. *Water* **11**, 1529. <https://doi.org/10.3390/w11081529>.
- Pitt, R. 2004 Illicit discharge detection and elimination: a guidance manual for program development and technical assessments. In: *Water Permits Division, Office of Water and Wastewater, U.S. Environmental Protection Agency*.
- Rödel, S., Günthert, F. W. & Brüggemann, T. 2017 Investigating the impacts of extraneous water on wastewater treatment plants. *Water Sci. Technol.* **75**, 847–855. <https://doi.org/10.2166/wst.2016.570>.
- Schilperoot, R. P. S., Gruber, G., Flamink, C. M. L., Clemens, F. H. L. R. & Graaf, J. H. J. M. v. d. 2006 Temperature and conductivity as control parameters for pollution-based real-time control. *Water Sci. Technol.* **54**, 257–263. <https://doi.org/10.2166/wst.2006.744>.
- Schilperoot, R., Hoppe, H., de Haan, C. & Langeveld, J. 2013 Searching for storm water inflows in foul sewers using fibre-optic distributed temperature sensing. *Water Sci. Technol.* **68**, 1723. <https://doi.org/10.2166/wst.2013.419>.
- Schweiger, R. M. & Hassell, C. L. 2004 Rooting out infiltration/inflow. *Water Environ. Technol.* **16**, 114–118.
- SMHI 2017 SMHI Öppna Data | Meteorologiska Observationer (SMHI Open Data | Meteorological Observations) [WWW Document]. SMHI Swed. Meteorol. Hydrol. Inst. Available from: <https://www.smhi.se/data/meteorologi/ladda-ner-meteorologiska-observationer> (accessed 6 May 2017).
- Sola, K. J., Bjerkholt, J. T., Lindholm, O. G. & Ratnaweera, H. 2020 Analysing consequences of infiltration and inflow water (I/I-water) using cost-benefit analyses. *Water Sci. Technol.* **82** (7), 1312–1326.
- Stauer, P., Scheidegger, A. & Rieckermann, J. 2012 Assessing the performance of sewer rehabilitation on the reduction of infiltration and inflow. *Water Res.* **46**, 5185–5196. <https://doi.org/10.1016/j.watres.2012.07.001>.
- Svenskt Vatten 2006 TV-inspektion av avloppsledningar i mark, P93 (CCTV-inspection of sewers in the ground, P93) (No. P93).
- Uusijärvi, J. 2013 Minskning av in- och utläckage genom aktiv läcksökning (Reduction of inflow and outflow through active leak detection) (No. 2013–03), Svenskt Vatten Utveckling.
- Wittenberg, H. & Aksoy, H. 2010 Groundwater intrusion into leaky sewer systems. *Water Sci. Technol.* **62**, 92. <https://doi.org/10.2166/wst.2010.287>.
- Wright, L., Heany, J. & Dent, S. 2006 Prioritizing sanitary sewers for rehabilitation using least-cost classifiers. *J. Infrastruct. Syst.* **12**, 174–183. <https://doi.org/10.1016/j.tree.2006.02.003>.
- Zhang, M., Liu, Y., Dong, Q., Hong, Y., Huang, X., Shi, H. & Yuan, Z. 2018a Estimating rainfall-induced inflow and infiltration in a sanitary sewer system based on water quality modelling: which parameter to use? *Environ. Sci. Water Res. Technol.* **4**, 385–393. <https://doi.org/10.1039/C7EW00371D>.
- Zhang, M., Liu, Y., Cheng, X., Zhu, D. Z., Shi, H. & Yuan, Z. 2018b Quantifying rainfall-derived inflow and infiltration in sanitary sewer systems based on conductivity monitoring. *J. Hydrol.* **558**, 174–183.

First received 11 January 2022; accepted in revised form 12 April 2022. Available online 6 May 2022